

Composite Cathodes Containing SWCNT@S Coaxial Nanocables: Facile Synthesis, Surface Modification, and Enhanced Performance for Li-Ion Storage

Shu-Mao Zhang, Qiang Zhang,* Jia-Qi Huang, Xiao-Fei Liu, Wancheng Zhu, Meng-Qiang Zhao, Wei-Zhong Qian, and Fei Wei

The arrangement and construction of 1D carbon nanotubes (CNTs) into frameworks with two or more levels of structures is an essential step to demonstrate their intrinsic properties and promising applications for energy storage. Single-walled CNTs (SWCNTs) are considered to have more excellent properties compared with multiwalled CNTs (MWCNTs), however, how to appropriately use SWCNTs as building blocks for nanocomposite electrodes is not well understood. Here, a composite cathode containing SWCNT@S coaxial nanocables for Li-S battery is fabricated by a facile melt-diffusion strategy. Beneficial from its sp^2 carbon nanostructure, higher specific surface area, larger aspect ratio, and interconnected electron pathway, the SWCNT@S cathode have reversible capacities of 676, 441 and 311 mAh g^{-1} for the first discharging at 0.5 C, 100th discharging at 1.0 C, and discharging at 10.0 C, respectively. These capacities are much higher than the corresponding capacities of the MWCNT@S cathode. By introducing polyethylene glycol (PEG) as a physical barrier to trap the highly polar polysulfide species, the PEG modified SWCNT@S cathode afforded improved reversible capacities. The cycling stability of the reversible capacities is expected to be further improved. The SWCNTs can serve as scaffolds for Li-S battery with much improved energy storage performance.

the carbon nanotubes (CNTs) exhibit excellent mechanical properties, electrical, and thermal conductivities, which facilitate their applications as electrode materials for high-voltage supercapacitors with high energy density and electron conductive fillers for Li-ion batteries.^[2] The graphene can also serve as both the template for the formation of electrochemical active materials and the current collector for efficient energy conversion and storage.^[3] Controllable introduction of electrochemical active materials into the CNT/graphene scaffold with tunable composition/structure and superior energy storage is a promising route to obtain new insight into materials science of nanocarbons and thus demonstrate their full potential for advanced energy storage.

Lithium batteries are very important for clean energy storage due to their high specific energy and good cycle life. Exploring cathode materials with high capacity to bypass the low performance of lithium-metal-oxide (LMO) cathode materials (e.g., $LiCoO_2$, $LiMnO_2$, $Li(Ni_{1/3}Co_{1/3}Mn_{1/3})O_2$, and $LiFePO_4$) is a great challenge for lithium batteries.^[4,5] Owing to the multiple-electron-transfer electrochemistry of light element-sulfur, the Li-S battery is with a high theoretical capacity and energy density of 1672 mAh g^{-1} and 2600 W h kg^{-1} , respectively.^[5,6] However, the insulating nature of S and Li_2S_x ($x = 1$ or 2), the low utilization of active phase, and the fast capacity degradation hinder the practical application of S cathode material. Novel electrolyte and advanced cathode materials are urgently anticipated to overcome these technical obstacles.

The incorporation of nanocarbons with high electronic conductivity, porous structure, and tunable surface area into sulfur cathode gives rise to advanced electrodes with improved capacity and cycling performance. For instance, Nazar and co-workers created highly ordered interwoven composites with mesoporous carbon CMK-3 that constrained sulfur within its channels and obtained a cathode with reversible capacities up to 1320 mAh g^{-1} .^[7] Porous carbon,^[7,8] activated carbon fiber,^[9] CNTs,^[10–15] and graphene^[16–18] were all demonstrated to be excellent fillers to improve the Li ion storage performance of S cathode.

With the rapid progresses on industrial mass production and commercialization of CNTs,^[19] validating the concept of CNTs

1. Introduction

The fine arrangement and construction of low-dimensional sp^2 nanocarbon (such as 1D nanotubes/wires/fibers, 2D graphene) into frameworks with two or more levels is an essential route for innovation of advanced energy materials.^[1,2] For instance,

S.-M. Zhang, Prof. Q. Zhang, Dr. J.-Q. Huang, X.-F. Liu, M.-Q. Zhao, Prof. W.-Z. Qian, Prof. F. Wei
Beijing Key Laboratory of Green Chemical Reaction Engineering and Technology
Department of Chemical Engineering
Tsinghua University
Beijing, 100084, China
E-mail: zhang-qiang@mails.tsinghua.edu.cn
X.-F. Liu, Prof. W. Zhu
Department of Chemical Engineering
Qufu Normal University
Shandong, 273165, China



DOI: 10.1002/ppsc.201200082

as the framework for advanced Li-S batteries is highly attractive. For instance, an initial discharge capacity of elemental sulfur positive electrode prepared by mixing with 50% sulfur, 20% acetylene black, 20% MWCNTs, and 10% polyvinylidene fluoride (PVDF) is 485 mAh g⁻¹ at 2.0 V vs. Li/Li⁺.^[20] The sulfur-coated multiwalled carbon nanotube (MWCNT) composite showed a reversible capacity of 670 mAh g⁻¹.^[12] High discharge capacity of sulfur was attained at 712 mAh g⁻¹ (23 wt% S) and 520 mAh g⁻¹ (50 wt% S) on flexible nanostructured sulfur-CNTs at a current density of 6 A g⁻¹.^[21] Recently, a sulfur-MWCNT composite exhibits excellent performance with high specific capacity up to 1355 mAh g⁻¹ at the initial discharge capacity was available, which however decreased rapidly to 854 mAh g⁻¹ after 30 cycles.^[11] A nano-sulfur/MWCNT composite had the specific capacity of 1210 mAh g⁻¹ in the initial cycle at a current rate of 300 mA g⁻¹, which degraded to a reversible capacity of 810 mAh g⁻¹ after 30 cycles.^[10] A CNT nano/micro-sphere with collective effect of hierarchical architecture, as well as the existence of carboxyl functional groups, was assembled into a novel sulfur/carbon materials with large pores for excellent Li ion storage performance.^[13] A hollow carbon nanofiber-encapsulated sulfur electrode structure with a high specific capacity of about 1580 and 730 mAh g⁻¹ was observed at C/5 rate for the first and 150th cycles of charge/discharge was available.^[22] Compared to MWCNTs, SWCNTs always render better mechanical, thermal, and electrical properties, and thus are considered as extraordinary platforms to demonstrate their intrinsic fascinating properties for high-performance nanocomposites, high electron mobility components for electronics, and field-emission displays. However, the Li ion storage behavior of composite electrode comprised with SWCNTs and sulfur has not been fully explored yet.

Here, SWCNTs mass-produced by fluidized bed chemical vapor deposition (CVD) were used as scaffolds to fabricate composite cathode for Li-S battery. A composite cathode containing SWCNT@S coaxial nanocables is available. The Li ion storage performance of SWCNT@S is found to be greatly improved compared with MWCNT@S cathode prepared by same melt-diffusion procedure. To further improve the Li ion storage performance, polyethylene glycol (PEG) was used as a barrier to enhance the discharge capacity, improve the Coulombic efficiency, and inhibit the shuttle effect as well. The reason we selected PEG as the barrier was based on the fact that PEG could trap the highly polar polysulfide species by the interaction between the ether groups and polysulfides. The PEG modified SWCNT@S cathode afforded a reversible capacity of 1005, 639, and 413 mAh g⁻¹ for the 1st discharging at 0.5 C, 100th discharging at 1.0 C, and discharging at 10.0 C, respectively. The cycling stability of discharging capacities should be improved by excellent entrapment of S-containing compounds for Li storage during charge-discharge process.

2. Results and Discussion

2.1. The SWCNT@ S Coaxial Nanocables

The SWCNTs produced on layered double hydroxide catalyst are intercrossed with each other to construct an electronic

conductive route and interconnected 3D macropores.^[23] The SWCNTs are with a very high specified surface area of 798 m² g⁻¹. After the facile melt-diffusion process, a coaxial nanocable nanocomposite in which the SWCNTs were uniformly coated by sulfur was obtained. As shown in **Figure 1a**, the cables were embedded in a sulfur matrix. Most of the nanocables connected with each other into a sparse net, guaranteeing a good electron pathway in the as-obtained nanocomposites. Detailed structure of the nanocable was further confirmed by the arrows in **Figure 1b,c**. The amorphous sulfur was uniformly attached on the SWCNTs. Although the SWCNTs were present in bundle contributed by van der Waals interactions, the sulfur phase can still be well distributed into the bundle due to the capillary interaction during the melt-diffusion process. The signal of element sulfur was easily detected in the energy-dispersive X-ray spectroscopy (EDS) (**Figure S1**, Supporting Information). As determined by thermogravimetry, the amount of sulfur in the nanocable was ca. 55.6% (**Figure 1d**). Most of the sulfur existed as matrix, which were loaded into the SWCNT network and evaporated before 270 °C. Compared with the evaporation of pure sulfur, the weight loss peak of sulfur in SWCNT@S shifted to higher temperature range of 180–300 °C (**Figure 1d**), indicating the confinement effect of sulfur in the SWCNT network. The micropores and mesopores of the SWCNTs were occupied by sulfur (**Figure 1e,f**). Meanwhile, the decrease of the pore volume from 1.72 to 0.01 cm³ g⁻¹ as well as the specific surface area from 798 to 6.1 m² g⁻¹ reconfirmed the occupation of the meso/micropores within the SWCNTs by sulfur.

2.2. The Electrochemical Performance of SWCNT@ S Coaxial Nanocables

The Li ion storage performance of the SWCNT@S cathode was investigated by cyclic voltammogram (CV), galvanostatic charge-discharge, and electrochemical impedance spectroscopy (EIS) measurement. The CV measurement was conducted with a scan rate of 0.1 mV s⁻¹ with the voltage range from 1.5 to 3.0 V vs. Li/Li⁺. As shown in **Figure 2a**, there were two main reduction peaks at around 2.29 and 2.01 V during the first cathodic scan. The first reduction peak corresponded to the transformation of sulfur to lithium polysulfide (Li₂S_n, 4 ≤ n ≤ 8), while the second peak can be ascribed to the reduction of high order lithium polysulfides into lithium sulfides (Li₂S₂ and Li₂S) at a lower potential. In the subsequent anodic scan, two oxidation peaks at ca. 2.43 and 2.52 V were observed. The first one was associated with the conversion from lithium sulfide to lithium polysulfide, and the second peak corresponded to the oxidation of the polysulfide into element sulfur. Both the reduction and oxidation peaks slightly shifted with the increase of cycle number, revealing a strong polarization of the electrode materials in the first cycle and the improvement of reversibility of the cell by cycling. In the second cathodic scan, the peaks of sulfur to lithium polysulfide shifted to 2.30 V, and intensity decreased a bit. In contrast, the intensity of the peaks corresponded to the reduction of higher order lithium polysulfide at 2.00 V significantly increased. Notably, no obvious change on the intensity and position of the anodic scan was observed except for the ratio of the oxidation of the lithium sulfide to

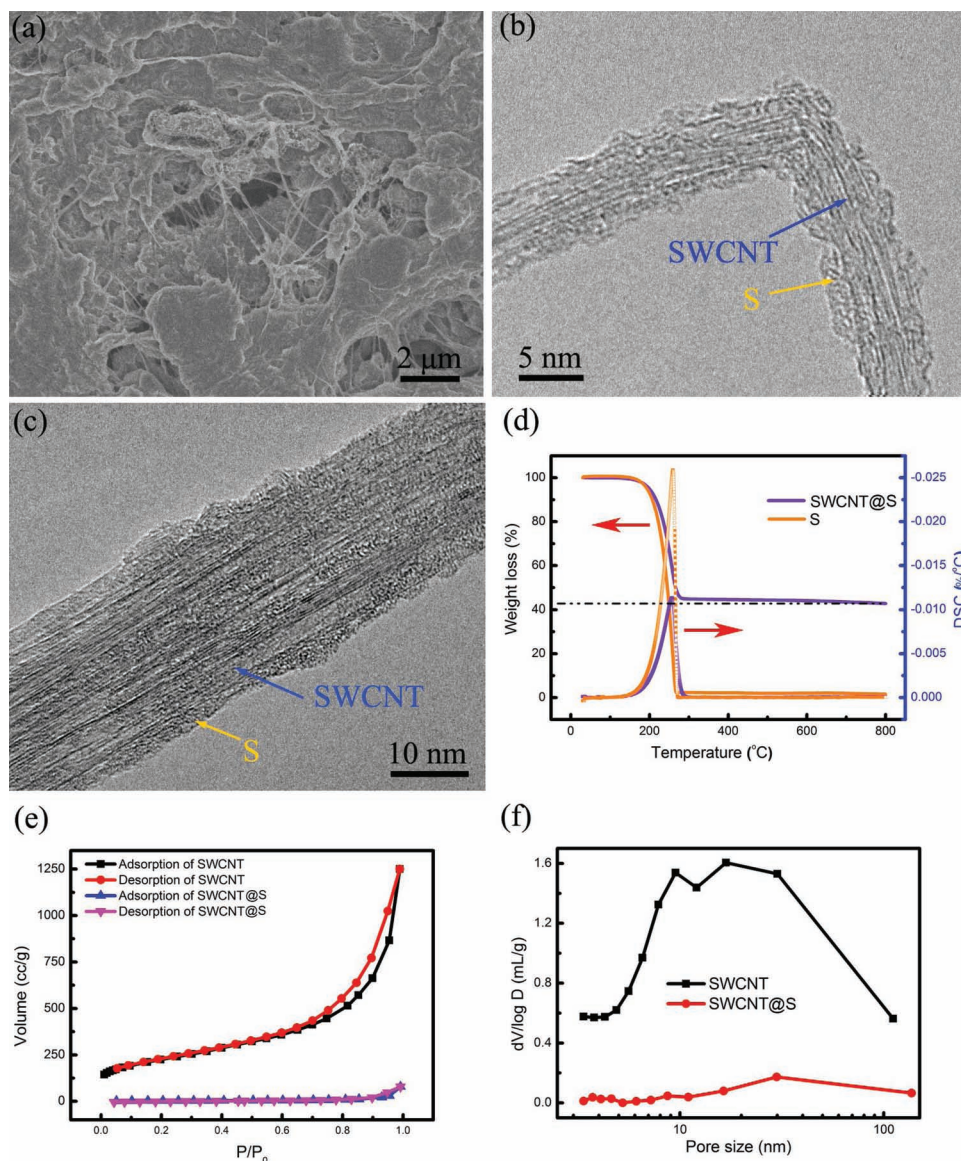


Figure 1. a) Scanning electron microscopy (SEM) images and b,c) transmission electron microscopy (TEM) images, d) TGA-DSC profile, e) N_2 sorption isotherm, and f) pore size distribution of the composite cathode containing SWCNT@S coaxial nanocables.

polysulfide. In the following CV test of cycle 3–5, the currents hardly changed, suggesting the good electrochemical reversibility for SWCNT@S cathode in Li storage.

Originated from the good electron pathway and effective combination of SWCNTs and S, the SWCNT@S cathode afforded an excellent rate capability, as indicated in Figure 2b. To demonstrate the proof-of-the-concept of SWCNT electrode, MWCNT@S cathode (Figure S2, Supporting Information) prepared by a similar melt-diffusion procedure was employed as the control sample. The SWCNT@S cathode offered a reversible capacity of 676 mAh g^{-1} at a current density of 0.5 C. This was larger than most reversible capacities of nanocarbon/sulfur electrode, such as MWCNT@S cathode (533 mAh g^{-1}), polymer wrapped sulfur particles (ca. 580 mAh g^{-1}),^[16] and graphene enveloped sulfur (ca. 550 mAh g^{-1} at 0.2 C).^[17] A

two-step discharging behavior was clearly observed, in which two typical plateaus at 2.31 and 2.06 V could be assigned to the two-step reaction of sulfur with lithium (Figure 2c). The positions of the plateaus were in accordance with the typical peaks of the SWCNT@S electrode shown in the CV profiles. There were also two plateaus in the charge process at about 2.24 and 2.36 V, respectively. Similar to other sulfur nanocomposite electrodes,^[10–16] the capacity decreased and the over-discharged phenomenon dramatically dwindled with the increase in the charge-discharge current density (Figure 2b,c). A very high current density of 10.0 C (16.7 A g^{-1}) was applied on the SWCNT@S and MWCNT@S electrode, while reversible capacities of 311 and 175 mAh g^{-1} were preserved, respectively (Figure 2b). However, the reversible capacity corresponding to the two typical plateaus decreased simultaneously. With the increase in the discharging

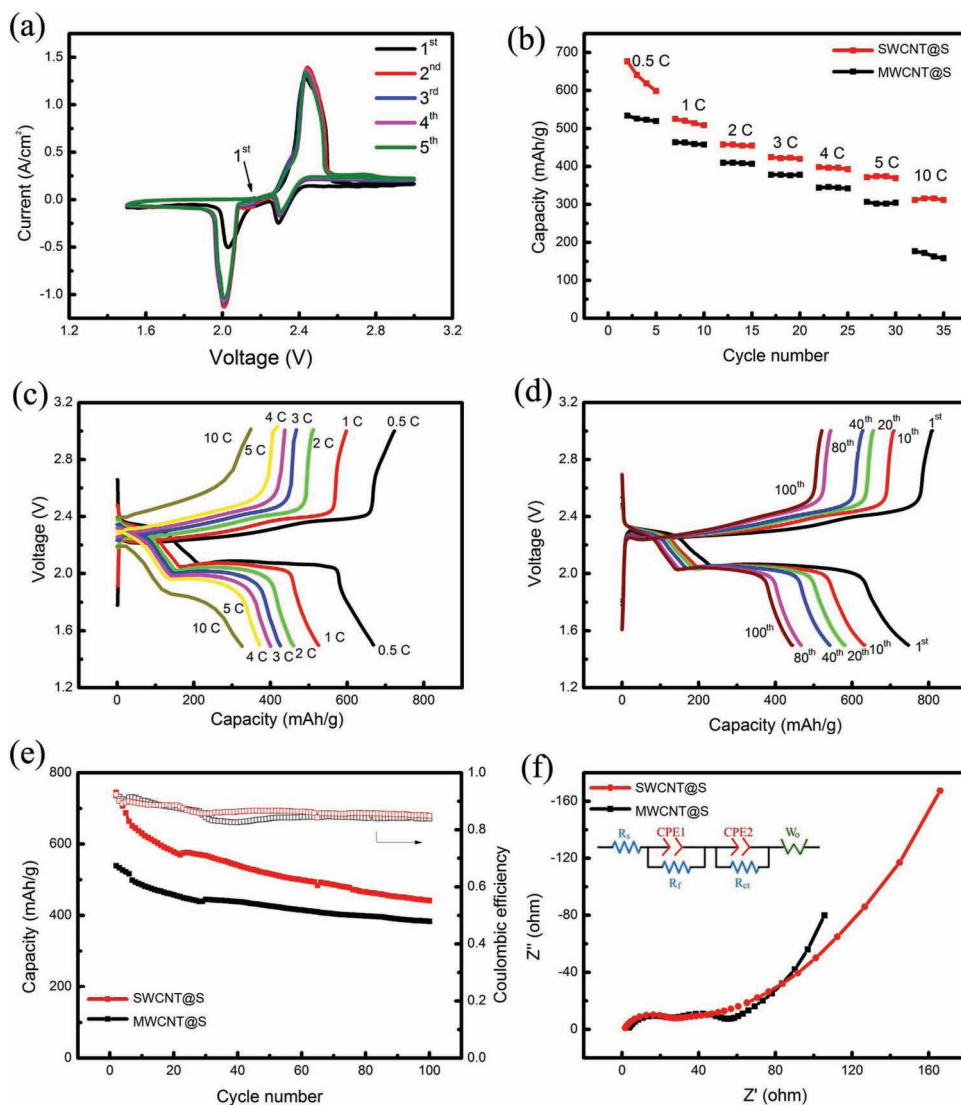


Figure 2. a) Cyclic voltammograms of the nanocomposite cathode containing SWCNT@S coaxial nanocables at 0.1 mV s^{-1} in the potential window from 1.5 to 3.0 V vs. Li^+/Li^0 . b) The rate capacity at different current densities of S/MWCNT@S coaxial nanocable. Galvanostatic charge-discharge curves of SWCNT@S coaxial nanocable cathode showing its c) rate and d) cycling dependent specific capacity. e) Cycling stability of S/MWCNT@S cathode at 1.0 C for 100 cycles. f) The Nyquist plot of S/MWCNT@S cathode.

current, the higher ordered lithium polysulfide reduction decayed rapidly, and polarization phenomena became significant. This can be partially attributed to the slow precipitation of Li_2S and Li_2S_2 on the SWCNT based cathode. The soluble polysulfide might also transfer through the separator and react with lithium anode, which was the so called shuttle effect. Such phenomena can be ambiguously detected on the galvanostatic charge-discharge curves of S/MWCNT@S coaxial nanocable cathode at different cycles (Figure 2d), in which the Coulombic efficiency did not reach 100%. The reversible capacity decay of either SWCNT@S or MWCNT@S cathode was observed. After 100 cycles, reversible capacities of 441 and 383 mAh g^{-1} were maintained on SWCNT@S and MWCNT@S nanocomposite electrode, respectively. A rapid capacity decay was observed at the beginning of the charge-discharge process, and the decay

tended to slow down. The reduction of sulfur and lithium polysulfide, as well as the oxidation of lithium sulfide and lithium polysulfide on pro-rata basis (Figure 2d), confirmed the loss of sulfur during the charge-discharge process.

It should be noticed that the SWCNT electrodes always render a higher Li storage capacity compared with that of MWCNTs. The SWCNTs were with higher specific surface area and better graphitization, which ensured the cable cathode better electron conductivity. This was further confirmed by the EIS spectra of S/MWCNT@S, as shown in Figure 2f. R_s , R_f and R_{ct} are impedances (resistances) due to electrolyte and cell components, surface film (electrolyte-electrode interface), and charge transfer (ct), respectively. CPEi is the respective constant phase element to account for the depressed semicircle in the experimental spectra. W_0 is the finite length Warburg (short circuit terminus)

Table 1. The summary of internal components in the CNT/S based cathode.

Cathode	R_s [Ω]	CPE1 [μ F]	R_f [Ω]	CPE2 [μ F]	R_{ct} [Ω]	W_o [Ω s ^{0.5}]
MWCNT@S	4.03	2.52	19.84	113.3	25.38	0.041
SWCNT@S	1.92	2.34	20.76	116.3	19.54	0.019
PEG-SWCNT@S	7.52	0.34	21.69	4.4	27.31	0.035

element related to the diffusion of lithium ions into the bulk cathode.^[24] The fitting results indicated that the R_s and R_{ct} of the SWCNT@S cathode were only 1.92 and 19.54 Ω , while those of MWCNT@S cathode were around 4.03 and 25.38 Ω , respectively (Table 1). The W_o of SWCNT@S was 0.019 Ω s^{0.5}, while that of MWCNT@S was 0.046 Ω s^{0.5}. Therefore, it can be concluded that Li ion diffusion resistance in the SWCNT@S cathode was smaller than that of MWCNT@S cathode.

In the SWCNT@S nanocable, the sulfur phase is distributed as the outer layer. Therefore, the leaching of lithium polysulfide is an important aspect for capacity loss. Thus, developing an efficient and effective way to sustain the shuttle of the S-containing compound by material structure design and battery pattern is urgently required. On one hand, the addition of LiNO₃ into the electrolyte helps the formation of solid electrolyte interface at both the cathode and anode. As a result, the polysulfide prefers to fully deposit on the cathode, leading to the increase of both the Coulombic efficiency and the discharging capacity.^[25] However, the loss of active S phase is not fully inhibited yet. On the other hand, the use of barrier to retard the shuttle of

S-containing compounds is a promising way to improve the capacity and stability of the composite cathode.

2.3. Surface Modification of SWCNT@S Coaxial Nanocable by PEG

To improve the Li storage performance of the SWCNT@S cathode, PEG was introduced on the surface of SWCNT@S cathode. As shown in Figure 3a, a very strong absorbance at 1097 cm⁻¹ was observed by infrared spectrometry (IR), indicating the occurrence of ether groups on the surface of SWCNT@S cathode. PEG layer was uniformly coated on the surface of SWCNT@S cathode, which was further confirmed by the SEM and TEM images shown in Figure 3. The surface of the PEG modified SWCNT@S particles became smooth (Figure 3b), and the SWCNTs still intercrossed into the S matrix. The thickness of the amorphous layers on the SWCNTs became larger. In some cases, a continuous polymer layer could be observed, revealing the presence of PEG. At the same time, a high amount of carbon and oxygen elements could be determined by the EDS analysis (Figure S1, Supporting Information). Such a PEG modified SWCNT@S cathode is expected to improve the Li ion storage performance of SWCNT@S cathode.

2.4. Enhanced Li-Ion Storage Performance

The CV profiles of the PEG modified SWCNT@S cathode are shown in Figure 4a. The main reduction peaks were observed at around 2.31 and 2.06 V during the first cathodic scan, and a very

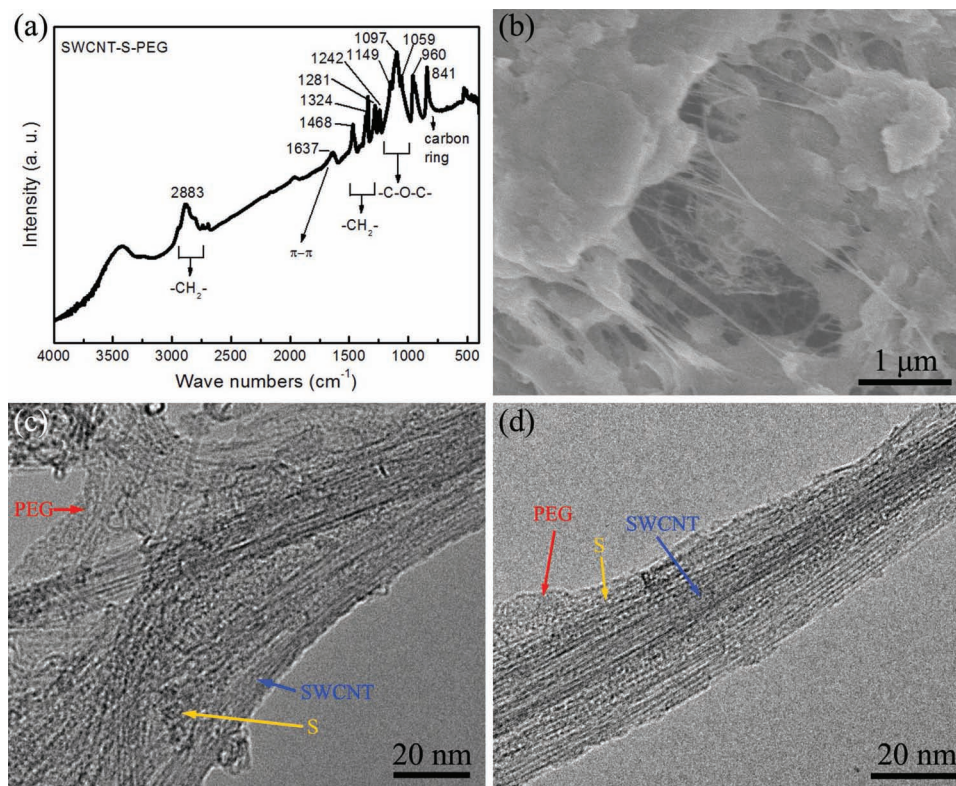


Figure 3. a) IR spectrum, b) SEM and c,d) TEM images of PEG modified nanocomposite cathode containing SWCNT@S coaxial nanocables.

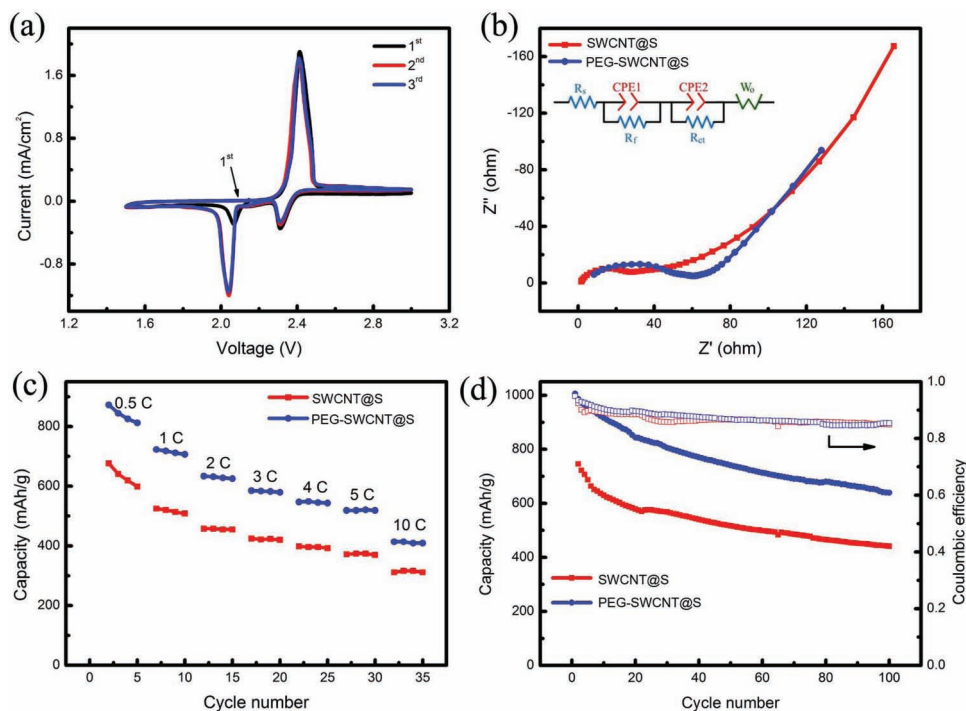


Figure 4. a) Cyclic voltammograms of the PEG-modified composite cathode containing SWCNT@S coaxial nanocables at 0.1 mV s^{-1} in the potential window from 1.5 to 3.0 V vs. Li^+/Li^0 . b) The Nyquist plot of PEG modified SWCNT@S cathode. c) The rate capacity at different current densities of PEG-modified S/MWCNT@S cathode. d) The cycling stability of S/MWCNT@S coaxial nanocable cathode at 1.0 C for 100 cycles.

strong oxidation peak at ca. 2.4 V was detected. The position of the lithium polysulfide shifted to 2.04 V during the followed cycles, while the intensity of both the reduction and oxidation peaks remained constant, demonstrating the good recycling of Li-ions. As shown in the EIS spectra (Figure 4b), the value of R_s , R_f , and R_{ct} obviously increased (Table 1), indicating the increase of the resistance of the electrolyte and cell components, surface film, and charge transfer (ct). The W_0 was also increased, revealing the Li-ion diffusion turned slow with the addition of PEG layer. In contrast, the CPE1 and CPE2 decreased obviously, indicating the capacitive performance decreased greatly. The reversible capacity obviously increased (Figure 4c). The reversible capacity of the SWCNT@S cathode increased from 745 to 1005 mAh g^{-1} after the PEG modification. The PEG modified composite can offer up to near 60% of the theoretical capacity of sulfur, much higher than that of the bare SWCNT@S cathode (44% utilization of the sulfur). Such an obvious increase in reversible capacity by PEG modification has been noticed in OMC/S and graphene/S nanocomposite cathode. Generally, polysulfide species are of high solubility in the ethereal solvents due to the solvation in ether-containing organic liquid, and the use of low viscous ethereal solvent results in a more complete reduction of soluble polysulfides.^[26] Herein, with the addition of PEG, the surface of SWCNT@S cathode became highly hydrophilic and a lot of ether group were exposed on the cathode surface. Therefore, a chemical gradient was constructed that the polysulfides would preferentially be trapped by ether groups on the cathode surface instead of dissolved in the bulk electrolyte. The concentration of polysulfide in the electrolyte inclines to be lower, and the redox shuttle mechanism is partially inhibited.^[7]

As a result, the deposition of insoluble sulfur species on the surface of the Li electrode and formation of irreversible Li_2S on the cathode surface are minimized. It is suspected that other additives with ether group and hydrophilic surface can also minimize the dissolution and diffusion of polysulfides,^[7,16] which is a facile way to greatly improve the cathode performance.

However, the capacitance decay was still observed. After 100 cycles, the reversible capacities of SWCNTs@S and PEG modified composite were 441 and 639 mAh g^{-1} , which corresponded to 59.2 and 63.6% of their first discharging capacity, respectively. A 0.36% capacitance loss per cycle was observed for the PEG modified SWCNT@S cathode, which is obviously lower than that of MWCNTs/S cathode (0.63%,^[12] 0.67%,^[15] 0.76%,^[20] 1.1%,^[10] or 1.2%^[11] per cycle), PEG-OMC/S cathode (1.7% per cycle),^[7] graphene/S cathode (0.96% per cycle),^[18] and competitive to the recent result on graphene/S composite by wrapping PEG (0.34% per cycle) and graphene-enveloped S (0.38% per cycle).^[16] Both the SWCNTs, modified graphene and graphene-enveloped S cathode show the slowest decay rate, which is suspected to be benefited from their high surface area and confinement effect for polysulfide dissolution/diffusion. In detail, there were still two plateaus on the galvanostatic discharge profiles at 2.31 and 2.06 V, respectively (Figure S3, Supporting Information). A monotonous loss of the two plateaus was detected. The gradual capacity decay was not fully solved yet, even though the capacity of PEG modified cathode offered a high reversible capacity. Exploring a way to improve the stability by minimizing the loss of active materials and electrolyte and optimizing the materials processing and cell design for robust Li-S battery with excellent stability are still highly required.

In addition, the rate performance of the PEG modified SWCNT@S was confirmed by Figure 4d. The reversible capacity of the unmodified and modified SWCNT@S cathode were 676 and 872 mAh g⁻¹ at 0.5 C, 311 and 413 mAh g⁻¹ at 10.0 C, respectively. Such a composite electrode is quite a promising electrode for Li-S battery with excellent performance in the area of energy storage.

3. Conclusions

A nanocomposite cathode containing SWCNT@S coaxial nanocables with a 1st reversible capacity of 676 mAh g⁻¹ at 0.5 C, a 100th reversible capacity of 441 mAh g⁻¹ at 1.0 C and 311 mAh g⁻¹ at 10.0 C was fabricated by a facile one-step melt-diffusion strategy. This is much higher than that of MWCNT@S with a 1st reversible capacity of 533 mAh g⁻¹ at 0.5 C, a 100th reversible capacity of 383 mAh g⁻¹ at 1.0 C, and a reversible discharging capacity of 175 mAh g⁻¹ at 10.0 C, respectively. Compared with MWCNTs, the SWCNTs were with better sp² carbon nanostructure, higher specific surface area, larger aspect ratio, and interconnected electron pathway, which made it a better scaffold for advanced cathode materials. However, owing to the shuttle effect of polysulfide, the rapid decay of discharging capacity was observed. PEG was introduced to modify the surface of the SWCNT@S nanocables. The PEG modified SWCNT@S cathode afforded a 1st reversible capacity of 1005 mAh g⁻¹ at 0.5 C, a 100th reversible capacity of 639 mAh g⁻¹ at 1.0 C, and a reversible discharging capacity of 413 mAh g⁻¹ at 10.0 C. The SWCNTs are promising scaffolds for Li-S battery with much improved property, and the as-obtained composite which contains CNTs based coaxial nanocables is a novel structural platform for the design of advanced functional materials with robust electron and thermal conductive pathway for energy storage, catalysts, and other applications.

4. Experimental Section

Preparation of SWCNT@S Coaxial Nanocable: The SWCNTs were grown on a Fe/Mg/Al LDH flakes in a fluidized bed reactor. The Fe/Mg/Al LDH flakes (*n*(Fe):*n*(Mg):*n*(Al) = 0.4:3:1) were prepared via a urea assisted co-precipitation reaction. During CVD growth, the quartz fluidized bed reactor was heated to 900 °C in Ar atmosphere at a flow rate of 500 mL min⁻¹. H₂ with a flow rate of 50 mL min⁻¹ was introduced into the reactor to start the reduction. After 5 min, the flow rate of Ar was turned down to 100 mL min⁻¹ and CH₄ (400 mL min⁻¹) was introduced into the fluidized bed reactor, starting the reaction occurred on the surface of the LDH flakes. The carbon product was then collected after the growth procedure. SWCNT products with a carbon purity of 99.5% were available after purification by HCl and NaOH leaching subsequently. The nanocomposite cathode containing SWCNT@S coaxial nanocables was fabricated by a facile melt-diffusion strategy as follows: Firstly, the SWCNTs and sulfur powder were mixed by milling and was placed uniformly in a sealed Teflon container at 155 °C for 3.0 h. Secondly, most of large sulfur particle was removed by heating in a quartz tube reactor with Ar flow.

Preparation of PEG Modified SWCNT@S Coaxial Nanocable: The PEG-20000 was dissolve in purified deionized water. The SWCNT@S cathode was soaked into the PEG-20000 solution for 24.0 h. Then the as obtained products were freeze dried for 3 days. The ratio of PEG introduced into S/MWCNT@S cathodes were both around 10.1 wt%.

Characterization: The electrodes were characterized using a JSM 7401F (JEOL Ltd., Tokyo, Japan) SEM and a JEM 2010 (JEOL Ltd., Tokyo, Japan) TEM. EDS analysis was performed using a JEM 2010 apparatus with the analytical software INCA, and the accelerating voltage applied was 120.0 kV. The sulfur content was obtained by TGA heated at 10 °C min⁻¹ using TGA/DSC1 STAR^e system with N₂ atmosphere. The BET specific surface area of all samples was measured by N₂ adsorption at liquid-N₂ temperature using Autosorb-iQ₂-MP-C system. Before measurements, the sample was degassed at 50 °C until a manifold pressure of 2 mm Hg was reached. It is not feasible to degas the sulfur composite at high temperature due to the possibility of sulfur sublimation. Pore size distribution plots were obtained by the Barrett-Joyner-Halenda method. The IR spectrum of PEG modified SWCNT@S composite cathode was collected using a Nicolet 6700 spectrometer.

Li-Ion Storage Performance: A slurry was first made by mixing the SWCNT@S coaxial nanocable active material with PVDF binder in NMP with a mass ratio of SWCNT@S:PVDF = 90:10. The slurry was vigorously magnetic stirred for ca. 18.0 h, leading to the homogeneously mixed slurry, which was coated on an Al foil, and then dried in a vacuum drying oven at 60 °C for 12.0 h. Subsequently, the foil was punched into disks with a diameter of 13 mm for the working electrodes. The electrode loading of SWCNT@S, MWCNT@S, PEG-SWCNT@S, and PEG-MWCNT@S cathode were 0.46, 0.48, 0.68, 0.69 mg cm⁻², respectively. The electrodes were assembled in a two-electrode cells configuration using standard 2025 coin-type cells versus Li metal foil as counter electrodes (1 mm thick), 1,3-dioxolane (DOL):1,2-dimethoxyethane (DME) (v/v = 1/1) with 1 mol L⁻¹ LiTFSI as the electrolyte, and the Celgard 2400 polypropylene membranes as separators. The electrode preparation and assembling of the coin-type cells were carried out in an Ar-filled glove box equipped with a purifying system with oxygen and water content below 1 ppm. The coin cells were tested in galvanostatic mode at various currents at 25 °C within a voltage range of 1.5–3.0 V using Neware multichannel battery cycler. The cyclic voltammogram and electrochemical impedance spectra measurements were performed on Solartron 1470E electrochemical workstation at a scan rate of 0.1 mV s⁻¹.

Supporting Information

Supporting Information is available from the Wiley Online Library or from the author.

Acknowledgments

The work was supported by the Foundation for the National Basic Research Program of China (973 Program, 2011CB932602).

Received: September 21, 2012

- [1] a) M. Q. Zhao, Q. Zhang, J. Q. Huang, F. Wei, *Adv. Funct. Mater.* **2012**, *22*, 675; b) R. T. Lv, T. X. Cui, M. S. Jun, Q. Zhang, A. Y. Cao, D. S. Su, Z. J. Zhang, S. H. Yoon, J. Miyawaki, I. Mochida, F. Y. Kang, *Adv. Funct. Mater.* **2011**, *21*, 999; c) C. de las Casas, W. Z. Li, *J. Power Sources* **2012**, *208*, 74.
- [2] a) D. S. Su, R. Schlogl, *ChemSusChem* **2010**, *3*, 136; b) C. Liu, F. Li, L. P. Ma, H. M. Cheng, *Adv. Mater.* **2010**, *22*, E28.
- [3] a) S. J. Guo, S. J. Dong, *Chem. Soc. Rev.* **2011**, *40*, 2644; b) Y. Q. Sun, Q. O. Wu, G. Q. Shi, *Energy Environ. Sci.* **2011**, *4*, 1113.
- [4] a) P. G. Bruce, B. Scrosati, J. M. Tarascon, *Angew. Chem. Int. Ed.* **2008**, *47*, 2930; b) J. B. Goodenough, Y. Kim, *Chem. Mater.* **2010**, *22*, 587.

- [5] N. S. Choi, Z. H. Chen, S. A. Freunberger, X. L. Ji, Y. K. Sun, K. Amine, G. Yushin, L. F. Nazar, J. Cho, P. G. Bruce, *Angew. Chem. Int. Ed.* **2012**, *51*, 9994.
- [6] P. G. Bruce, S. A. Freunberger, L. J. Hardwick, J. M. Tarascon, *Nat. Mater.* **2012**, *11*, 19.
- [7] X. L. Ji, K. T. Lee, L. F. Nazar, *Nat. Mater.* **2009**, *8*, 500.
- [8] a) J. Schuster, G. He, B. Mandlmeier, T. Yim, K. T. Lee, T. Bein, L. F. Nazar, *Angew. Chem. Int. Ed.* **2012**, *51*, 3591; b) G. He, X. L. Ji, L. Nazar, *Energy Environ. Sci.* **2011**, *4*, 2878; c) D. W. Wang, G. M. Zhou, F. Li, K. H. Wu, G. Q. Lu, H. M. Cheng, I. R. Gentle, *Phys. Chem. Chem. Phys.* **2012**, *14*, 8703.
- [9] R. Elazari, G. Salitra, A. Garsuch, A. Panchenko, D. Aurbach, *Adv. Mater.* **2011**, *23*, 5641.
- [10] J. J. Chen, X. Jia, Q. J. She, C. Wang, Q. A. Zhang, M. S. Zheng, Q. F. Dong, *Electrochim. Acta* **2010**, *55*, 8062.
- [11] W. Ahn, K. B. Kim, K. N. Jung, K. H. Shin, C. S. Jin, *J. Power Sources* **2012**, *202*, 394.
- [12] L. X. Yuan, H. P. Yuan, X. P. Qiu, L. Q. Chen, W. T. Zhu, *J. Power Sources* **2009**, *189*, 1141.
- [13] J. J. Chen, Q. Zhang, Y. N. Shi, L. L. Qin, Y. Cao, M. S. Zheng, Q. F. Dong, *Phys. Chem. Chem. Phys.* **2012**, *14*, 5376.
- [14] a) S. Dorfler, M. Hagen, H. Althues, J. Tubke, S. Kaskel, M. J. Hoffmann, *Chem. Commun.* **2012**, *48*, 4097; b) W. Wei, J. L. Wang, L. J. Zhou, J. Yang, B. Schumann, Y. N. NuLi, *Electrochem. Commun.* **2011**, *13*, 399.
- [15] J. C. Guo, Y. H. Xu, C. S. Wang, *Nano Lett.* **2011**, *11*, 4288.
- [16] H. L. Wang, Y. Yang, Y. Y. Liang, J. T. Robinson, Y. G. Li, A. Jackson, Y. Cui, H. J. Dai, *Nano Lett.* **2011**, *11*, 2644.
- [17] S. Evers, L. F. Nazar, *Chem. Commun.* **2012**, *48*, 1233.
- [18] Y. L. Cao, X. L. Li, I. A. Aksay, J. Lemmon, Z. M. Nie, Z. G. Yang, J. Liu, *Phys. Chem. Chem. Phys.* **2011**, *13*, 7660.
- [19] Q. Zhang, J. Q. Huang, M. Q. Zhao, W. Z. Qian, F. Wei, *ChemSusChem* **2011**, *4*, 864.
- [20] S. C. Han, M. S. Song, H. Lee, H. S. Kim, H. J. Ahn, J. Y. Lee, *J. Electrochem. Soc.* **2003**, *150*, A889.
- [21] G. M. Zhou, D. W. Wang, F. Li, P. X. Hou, L. C. Yin, C. Liu, I. Gentle, G. Q. Lu, H. M. Cheng, *Energy Environ. Sci.* **2012**, *5*, 8901.
- [22] G. Y. Zheng, Y. Yang, J. J. Cha, S. S. Hong, Y. Cui, *Nano Lett.* **2011**, *11*, 4462.
- [23] a) M.-Q. Zhao, Q. Zhang, X.-L. Jia, J.-Q. Huang, Y.-H. Zhang, F. Wei, *Adv. Funct. Mater.* **2010**, *20*, 677; b) M.-Q. Zhao, Q. Zhang, J.-Q. Huang, J.-Q. Nie, F. Wei, *Carbon* **2010**, *48*, 3260.
- [24] C. J. Zhang, X. He, Q. S. Kong, H. Li, H. Hu, H. B. Wang, L. Gu, L. Wang, G. L. Cui, L. Q. Chen, *Cryst. Eng. Comm.* **2012**, *14*, 4344.
- [25] a) D. Aurbach, E. Pollak, R. Elazari, G. Salitra, C. S. Kelley, J. Affinito, *J. Electrochem. Soc.* **2009**, *156*, A694; b) X. Liang, Z. Y. Wen, Y. Liu, M. F. Wu, J. Jin, H. Zhang, X. W. Wu, *J. Power Sources* **2011**, *196*, 9839; c) S. S. Zhang, *Electrochim. Acta* **2012**, *70*, 344.
- [26] J. Gao, M. A. Lowe, Y. Kiya, H. D. Abruna, *J. Phys. Chem. C* **2011**, *115*, 25132.